

Linear optical universal quantum gates with higher success probabilities

Wen-Qiang Liu¹ and Hai-Rui Wei^{2,*}

1 Center for Quantum Technology Research and Key Laboratory of Advanced Optoelectronic Quantum Architecture and Measurements (MOE), School of Physics, Beijing Institute of Technology, Beijing 100081, China

2 School of Mathematics and Physics, University of Science and Technology Beijing, Beijing 100083, China

* hrwei@ustb.edu.cn

November 18, 2022

Abstract

Universal quantum gates lie at the heart of designing quantum computer. We construct two compact quantum circuits to implement post-selected controlled-phase-flip (CPF) gate and Toffoli gate with linear optics assisted by one and two single photons, respectively. The current existing maximum success probability of 1/4 for linear optical CPF gate is achieved by resorting to an ancillary single photon rather than an entangled photon pair or two single photons. Remarkably, our Toffoli gate is accomplished with current maximum success probability of 1/30 without using additional entangled photon pairs and the standard decomposition-based approach. Linear optical implementations of the presented two universal gates are feasible under current technology and provide a potential application in large-scale optical quantum computing.

Contents

1	Introduction	2
2	Post-selected CPF gate with linear optics	3
3	Post-selected Toffoli gate with linear optics	5
4	Conclusion	10
References		11

1 Introduction

Quantum computing [1] has the remarkable potential to dramatically surpass its classical counterpart on solving certain complex tasks in terms of the processing speed or resource overhead. Universal quantum gates are crucial building blocks in quantum circuit model [2–6], quantum algorithms [7–9], quantum simulations [10–12], quantum communication [13], and quantum computing [14–17]. Photon is generally viewed as one of the promising candidates for flying and solid-state quantum computing owing to its outstanding low decoherence, high-speed transmission, natural information carrier, flexible single-qubit manipulations, and available atom-like qubit interconnector [18, 19]. Strong interactions between individual photons are the key resources for nontrivial multi-photon quantum gates, and the prohibited photon-photon interactions can be remedied efficiently by using linear optics [20] or solid-state media [21–23]. Unfortunately, solid-state platforms are challenged by inefficiency and imperfection in experiments. The probabilistic character of universal quantum gates with linear optics is unavoidable. Hence, minimizing the quantum resources required to implement quantum gates with higher success probability is a central problem of linear optical quantum computing, and tremendous efforts have been made on it [24–39].

Controlled phase flip (CPF) gate or its equivalent controlled-NOT (CNOT) gate is the most quintessential universal quantum gate [1]. CNOT gates together with single-qubit rotations are sufficient to implement any quantum computation [2]. Nowadays, CNOT gate has been experimentally demonstrated in several physical systems [40–42]. The KLM scheme [20] is served as a stepping stone for implementing CPF gate with a sheer number of linear optics, large and good quantum memory, and giant interferometer phase stable. Various improved works were later proposed both in theory and experiment [24–39]. So far, it has been demonstrated that CPF gate can be completed with a success probability of $1/9$, which is the existing maximum value achievable without ancillary photons [30–35], and the success probability can be improved to $1/8$ via two additional independent single photons [36, 37]. The current existing highest success probability of $1/4$ for a CNOT gate has been achieved assisted by a necessary entangled photon pair [25–29]. Deterministic generation of entangled photon pairs based on spontaneous parametric down-conversion remains a key technical obstacle in experiments due to multi-photon emissions and probabilistic properties [43].

Toffoli gate supplemented with Hadamard gate can simulate any multi-qubit quantum computing [1]. Toffoli gate is also served as an essential part in quantum factoring algorithm [44], quantum search algorithm [45], quantum half-adder [46], quantum error correction [47], and quantum fault tolerance [48], etc. Much attention has been paid to the realization of Toffoli gate [49–51]. It has been confirmed theoretically that the optimal cost of a Toffoli gate is six CNOT gates [2] or five two-qubit entangling gates [52]. Such synthesis might be helpful to design complex quantum gate, but it makes the gate further susceptible to the environmental noise and increases the time scale of the system. Without using the standard decomposition-based approach, early in 2006, Fiurášek [53] first showed a three-photon polarization Toffoli gate with a success probability of 0.75% (approximately $1/133$) using linear optics. Using higher-dimensional Hilbert spaces, Ralph *et al.* [54] improved the success probability of a linear optical Toffoli gate to $1/72$ in 2007, and this interesting probabilistic scheme was later experimentally demonstrated in 2009 [55]. Recently, Liu *et al.* [56] further enhanced the success probability of the Toffoli gate to $1/64$. In the same year, a post-selected Toffoli gate with a success probability of $1/60$ was experimentally realized on a programmable silicon-

based photonic chip [57]. Additionally, in 2022, Li *et al.* [58] experimentally demonstrated a path-based three-photon Toffoli gate with a success probability of 1/72. Many hybrid multiple degrees of freedom (DOFs) probabilistic and deterministic Toffoli gates were also reported in recent years [59–63].

In this paper, we propose two compact quantum circuits to implement post-selected CPF and Toffoli gates in the coincidence basis using solely polarizing beam splitters (PBSs), half-wave plates (HWPs), beam splitters (BSs), and single-photon detectors. Assisted by one and two independent single photons, our CPF and Toffoli gates are accomplished respectively when exactly one photon appears in each output mode. Our schemes are appealing for higher success probabilities and less quantum resource requirements. The existing highest success probability of a linear optical CPF gate 1/4 is achieved resorting to an auxiliary single photon in our scheme rather than an auxiliary entangled photon pair [25–29]. The presented CPF gate also beats the ones with the success probability of 1/8 assisted by two single photons [36, 37], and the ones with 1/9 without auxiliary photons [30–35]. In addition, the average success probability of our Toffoli gate is high to 1/30, which far exceeds all previous results for the same works [53–56].

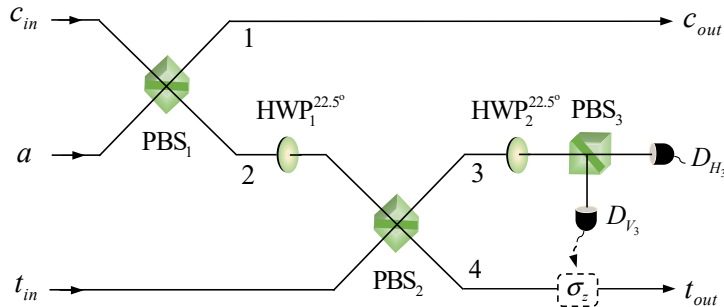


Figure 1: Schematic diagram of a post-selected CPF gate. The gate is completed in case each spatial modes 1, 3 and 4 contain exactly one photon. PBS, a polarizing beam splitter, transmits the H -polarized photon and reflects the V -polarized photon. $\text{HWP}^{22.5^\circ}$, a half-wave plate setting at 22.5° , results in $|H\rangle \rightarrow \frac{1}{\sqrt{2}}(|H\rangle + |V\rangle)$ and $|V\rangle \rightarrow \frac{1}{\sqrt{2}}(|H\rangle - |V\rangle)$. D_{H_3} and D_{V_3} stand for the single-photon detectors. Feed-forward operation $\sigma_z = |H\rangle\langle H| - |V\rangle\langle V|$ is applied when D_{V_3} is triggered.

Our scheme described in Fig. 1 shows a polarization-based post-selected CPF gate can be completed in the following three steps.

First, the two gate photons and one auxiliary photon in the states

$$|\phi\rangle_{c_{in}} = \alpha_1|H\rangle_{c_{in}} + \beta_1|V\rangle_{c_{in}}, \quad (1)$$

$$|\phi\rangle_{t_{in}} = \alpha_2|H\rangle_{t_{in}} + \beta_2|V\rangle_{t_{in}}, \quad (2)$$

$$|\phi\rangle_a = \frac{1}{\sqrt{2}}(|H\rangle_a + |V\rangle_a), \quad (3)$$

are injected into the spatial modes c_{in} , t_{in} , and a , respectively. Here coefficients α_1 , β_1 , α_2 , β_2 satisfy the conditions $|\alpha_1|^2 + |\beta_1|^2 = 1$ and $|\alpha_2|^2 + |\beta_2|^2 = 1$. The subscripts denote the spatial modes of photons (also named photon's paths).

The photons emitted from spatial modes c_{in} and a are fed into PBS₁, simultaneously. PBS₁ transforms the state of the whole system from $|\Phi_1\rangle = |\phi\rangle_{c_{in}} \otimes |\phi\rangle_a \otimes |\phi\rangle_{t_{in}}$ to

$$\begin{aligned} |\Phi_2\rangle &= \frac{1}{\sqrt{2}}(\alpha_1|H\rangle_1|H\rangle_2 + \beta_1|H\rangle_1|V\rangle_1 + \alpha_1|H\rangle_2|V\rangle_2 + \beta_1|V\rangle_1|V\rangle_2) \\ &\otimes (\alpha_2|H\rangle_{t_{in}} + \beta_2|V\rangle_{t_{in}}). \end{aligned} \quad (4)$$

Based on Eq. (4), one can see that PBS₁ can complete a parity-check measurement on the polarization photons by choosing the instance in which each of the spatial mode contains exactly one photon in post-selection principle, and then the system would be changed into the state

$$|\Phi_3\rangle = (\alpha_1|H\rangle_1|H\rangle_2 + \beta_1|V\rangle_1|V\rangle_2) \otimes (\alpha_2|H\rangle_{t_{in}} + \beta_2|V\rangle_{t_{in}}), \quad (5)$$

with a probability of 1/2. While the instance in which each spatial mode involves two photons or none photon indicates the gate operation fails.

Second, as shown in Fig. 1, before and after the photons from modes 2 and t_{in} pass through PBS₂ simultaneously, two polarization Hadamard operations are performed on them by using HWP₁^{22.5°} and HWP₂^{22.5°}, respectively. Here half-wave plate oriented at 22.5° (HWP^{22.5°}) completes the transformations

$$|H\rangle \xrightarrow{\text{HWP}^{22.5^\circ}} \frac{1}{\sqrt{2}}(|H\rangle + |V\rangle), \quad |V\rangle \xrightarrow{\text{HWP}^{22.5^\circ}} \frac{1}{\sqrt{2}}(|H\rangle - |V\rangle). \quad (6)$$

Operations HWP₁^{22.5°} → PBS₂ → HWP₂^{22.5°} transform the state $|\Phi_3\rangle$ into

$$\begin{aligned} |\Phi_4\rangle &= \frac{1}{2}(\alpha_1\alpha_2|H\rangle_1|H\rangle_4 + \alpha_1\beta_2|H\rangle_1|V\rangle_4 + \beta_1\alpha_2|V\rangle_1|H\rangle_4 - \beta_1\beta_2|V\rangle_1|V\rangle_4)|H\rangle_3 \\ &+ \frac{1}{2}(\alpha_1\alpha_2|H\rangle_1|H\rangle_4 - \alpha_1\beta_2|H\rangle_1|V\rangle_4 + \beta_1\alpha_2|V\rangle_1|H\rangle_4 + \beta_1\beta_2|V\rangle_1|V\rangle_4)|V\rangle_3 \\ &+ \frac{1}{2\sqrt{2}}(\alpha_1\alpha_2|H\rangle_1 - \beta_1\alpha_2|V\rangle_1)(|H\rangle_3 + |V\rangle_3)(|H\rangle_3 - |V\rangle_3) \\ &+ \frac{1}{\sqrt{2}}(\alpha_1\beta_2|H\rangle_1 + \beta_1\beta_2|V\rangle_1)|H\rangle_4|V\rangle_4. \end{aligned} \quad (7)$$

We choose the case where exactly one photon in each of the spatial modes 3 and 4, and then the system would be in a normalization state

$$\begin{aligned} |\Phi_5\rangle &= \frac{1}{\sqrt{2}}(\alpha_1\alpha_2|H\rangle_1|H\rangle_4 + \alpha_1\beta_2|H\rangle_1|V\rangle_4 + \beta_1\alpha_2|V\rangle_1|H\rangle_4 - \beta_1\beta_2|V\rangle_1|V\rangle_4)|H\rangle_3 \\ &+ \frac{1}{\sqrt{2}}(\alpha_1\alpha_2|H\rangle_1|H\rangle_4 - \alpha_1\beta_2|H\rangle_1|V\rangle_4 + \beta_1\alpha_2|V\rangle_1|H\rangle_4 + \beta_1\beta_2|V\rangle_1|V\rangle_4)|V\rangle_3, \end{aligned} \quad (8)$$

with a probability of $\frac{1}{2} \times \frac{1}{2} = \frac{1}{4}$.

Finally, the photon emitted from spatial mode a will be detected by using PBS_3 and photon detectors D_{H_3} and D_{V_3} . Based on Eq. (8), one can see that when D_{H_3} is fired, the photons emitted from c_{out} and t_{out} kept are in the state

$$|\Phi_6\rangle = \alpha_1\alpha_2|H\rangle_1|H\rangle_4 + \alpha_1\beta_2|H\rangle_1|V\rangle_4 + \beta_1\alpha_2|V\rangle_1|H\rangle_4 - \beta_1\beta_2|V\rangle_1|V\rangle_4, \quad (9)$$

with a probability of $\frac{1}{4} \times \frac{1}{2}$. And then, the performance of CPF gate is completed.

When D_{V_3} is fired, the system will collapse into the state

$$|\Phi'_6\rangle = \alpha_1\alpha_2|H\rangle_1|H\rangle_4 - \alpha_1\beta_2|H\rangle_1|V\rangle_4 + \beta_1\alpha_2|V\rangle_1|H\rangle_4 + \beta_1\beta_2|V\rangle_1|V\rangle_4, \quad (10)$$

with a probability of $\frac{1}{4} \times \frac{1}{2}$. It is easily to convert Eq. (10) to Eq. (9) by applying a feed-forward σ_z operation on the photon emitted from spatial mode 4, which can be achieved by an HWP^{0° .

Putting all the pieces together, one can see that the quantum circuit shown in Fig. 1 completed a CPF operation conditional on exactly one photon in each of the output spatial modes. The total success probability of the presented gate can reach the current existing best result $\frac{1}{8} + \frac{1}{8} = \frac{1}{4}$, and only one additional single photon is required.

The scheme shown in Fig. 1 is actually the post-selection result, i.e., the gate success is heralded by simultaneous successful detection of exactly one photon for each qubit. Nowadays, the various schemes for realizing post-selected-based CPF gate [30–32] and CNOT gate [33–35] have been proposed and experimentally demonstrated. Our scheme surpasses them in terms of the success probability and the quantum resource cost.

3 Post-selected Toffoli gate with linear optics

Toffoli gate flips the state of the target qubit if the two controlled qubits both are in $|1\rangle$, and has no effect otherwise. Figure 2 depicts a scheme for implementing a Toffoli gate with an average success probability of $1/30$ in the linear optical system.

Suppose two controlled photons, one target photon, and two auxiliary photons are initially prepared in the following states

$$|\psi\rangle_{c1in} = \alpha_1|H\rangle_{c1in} + \beta_1|V\rangle_{c1in}, \quad (11)$$

$$|\psi\rangle_{c2in} = \alpha_2|H\rangle_{c2in} + \beta_2|V\rangle_{c2in}, \quad (12)$$

$$|\psi\rangle_{t_{in}} = \alpha_3|H\rangle_{t_{in}} + \beta_3|V\rangle_{t_{in}}, \quad (13)$$

$$|\psi\rangle_{a_1} = \frac{1}{\sqrt{2}}(|H\rangle_{a_1} + |V\rangle_{a_1}), \quad (14)$$

$$|\psi\rangle_{a_2} = \frac{1}{\sqrt{2}}(|H\rangle_{a_2} + |V\rangle_{a_2}), \quad (15)$$

where $|\alpha_1|^2 + |\beta_1|^2 = 1$, $|\alpha_2|^2 + |\beta_2|^2 = 1$, and $|\alpha_3|^2 + |\beta_3|^2 = 1$.

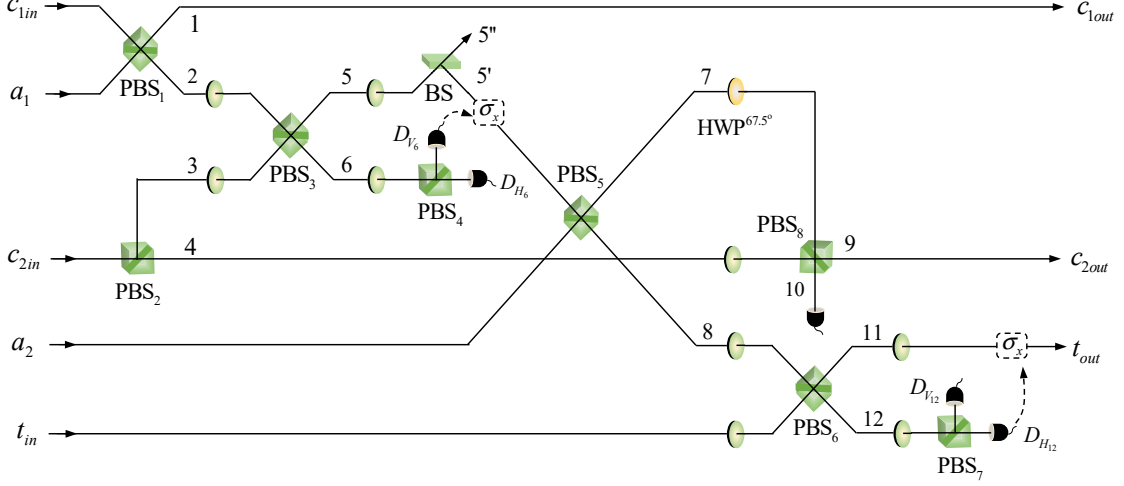


Figure 2: Schematic diagram of a post-selected Toffoli gate. The gate works successfully conditioned on exactly one photon in each spatial modes 6, 12, c_{1out} , c_{2out} , and t_{out} . BS, a 50:50 beam splitter, results in $|H\rangle_5 \rightarrow \frac{1}{\sqrt{2}}(|H\rangle_{5'} + |H\rangle_{5''})$ and $|V\rangle_5 \rightarrow \frac{1}{\sqrt{2}}(|V\rangle_{5'} + |V\rangle_{5''})$. HWP $^{67.5^\circ}$ completes the transformations $|H\rangle \rightarrow \frac{1}{\sqrt{2}}(-|H\rangle + |V\rangle)$ and $|V\rangle \rightarrow \frac{1}{\sqrt{2}}(|H\rangle + |V\rangle)$. Pauli operation $\sigma_x = |H\rangle\langle V| + |V\rangle\langle H|$ is applied when D_{V6} or D_{H12} is triggered, which is achieved by an HWP $^{45^\circ}$.

In the first step, we employ PBS₁ to complete the parity-check measurement on the first controlled photon (emitted from spatial c_{1in}) and the first additional photon (emitted from spatial a_1), and choose the instance in which each outing mode contains exactly one photon. And then, PBS₁ converts the whole system from the initial state $|\Psi_0\rangle = |\psi\rangle_{c_{1in}} \otimes |\psi\rangle_{a_1} \otimes |\psi\rangle_{c_{2in}} \otimes |\psi\rangle_{a_2} \otimes |\psi\rangle_{t_{in}}$ to

$$|\Psi_1\rangle = \frac{1}{\sqrt{2}}(\alpha_1|H\rangle_1|H\rangle_2 + \beta_1|V\rangle_1|V\rangle_2) \otimes (\alpha_2|H\rangle_{c_{2in}} + \beta_2|V\rangle_{c_{2in}}) \otimes (|H\rangle_{a_2} + |V\rangle_{a_2}) \otimes (\alpha_3|H\rangle_{t_{in}} + \beta_3|V\rangle_{t_{in}}), \quad (16)$$

with a probability of 1/2.

In the second step, PBS₂ transmits $H_{c_{2in}}$ -polarized component to PBS₈ and reflects $V_{c_{2in}}$ -polarized component to spatial mode 3 for mixing with the components emitted from spatial mode 2 at PBS₃. After the photons emitted from spatial modes 2 and 3 experience the block composed of four HWP $^{22.5^\circ}$ s and PBS₃, we choose the instance in which each of spatial modes 5 and 6 contains exactly one photon, and then the system will become the normalization state

$$\begin{aligned} |\Psi_2\rangle = & \frac{1}{2\sqrt{2}}[(\alpha_1\alpha_2|H\rangle_1|H\rangle_4|H\rangle_6 + \beta_1\alpha_2|V\rangle_1|H\rangle_4|H\rangle_6 + \alpha_1\alpha_2|H\rangle_1|H\rangle_4|V\rangle_6 \\ & + \beta_1\alpha_2|V\rangle_1|H\rangle_4|V\rangle_6 + \alpha_1\alpha_2|H\rangle_1|H\rangle_4|H\rangle_5 - \beta_1\alpha_2|V\rangle_1|H\rangle_4|H\rangle_5 \\ & - \alpha_1\alpha_2|H\rangle_1|H\rangle_4|V\rangle_5 + \beta_1\alpha_2|V\rangle_1|H\rangle_4|V\rangle_5) + \frac{1}{2}(\alpha_1\beta_2|H\rangle_1|V\rangle_5|H\rangle_6 \\ & + \beta_1\beta_2|V\rangle_1|H\rangle_5|H\rangle_6 + \alpha_1\beta_2|H\rangle_1|H\rangle_5|V\rangle_6 + \beta_1\beta_2|V\rangle_1|V\rangle_5|V\rangle_6)] \\ & \otimes (|H\rangle_{a_2} + |V\rangle_{a_2}) \otimes (\alpha_3|H\rangle_{t_{in}} + \beta_3|V\rangle_{t_{in}}), \end{aligned} \quad (17)$$

with a probability of $\frac{1}{2} \times \frac{1+\alpha_2^2}{2}$. In order to complete the Toffoli gate with unity fidelity in principle, we next reduce the amplitude of the photon emitted from spatial mode 5 to half by using a 50:50 beam splitter (BS). The unitary transformations of the BS can be described as

$$|H\rangle_5 \xrightarrow{\text{BS}} \frac{1}{\sqrt{2}}(|H\rangle_{5'} + |H\rangle_{5''}), \quad |V\rangle_5 \xrightarrow{\text{BS}} \frac{1}{\sqrt{2}}(|V\rangle_{5'} + |V\rangle_{5''}). \quad (18)$$

That is, BS yields the state

$$\begin{aligned} |\Psi_3\rangle = & \frac{1}{2\sqrt{2}}(\alpha_1\alpha_2|H\rangle_1|H\rangle_4 + \beta_1\alpha_2|V\rangle_1|H\rangle_4 + \alpha_1\beta_2|H\rangle_1|V\rangle_{5'} \\ & + \beta_1\beta_2|V\rangle_1|H\rangle_{5'} + \alpha_1\beta_2|H\rangle_1|V\rangle_{5''} + \beta_1\beta_2|V\rangle_1|H\rangle_{5''}) \\ & \otimes |H\rangle_6 \otimes (|H\rangle_{a_2} + |V\rangle_{a_2}) \otimes (\alpha_3|H\rangle_{t_{in}} + \beta_3|V\rangle_{t_{in}}) \\ & + \frac{1}{2\sqrt{2}}(\alpha_1\alpha_2|H\rangle_1|H\rangle_4 + \beta_1\alpha_2|V\rangle_1|H\rangle_4 + \alpha_1\beta_2|H\rangle_1|H\rangle_{5'} \\ & + \beta_1\beta_2|V\rangle_1|V\rangle_{5'} + \alpha_1\beta_2|H\rangle_1|H\rangle_{5''} + \beta_1\beta_2|V\rangle_1|V\rangle_{5''}) \\ & \otimes |V\rangle_6 \otimes (|H\rangle_{a_2} + |V\rangle_{a_2}) \otimes (\alpha_3|H\rangle_{t_{in}} + \beta_3|V\rangle_{t_{in}}) \\ & + \frac{1}{4}(\alpha_1\alpha_2|H\rangle_1|H\rangle_4|H\rangle_{5'} - \alpha_1\alpha_2|H\rangle_1|H\rangle_4|V\rangle_{5'} - \beta_1\alpha_2|V\rangle_1|H\rangle_4|H\rangle_{5'} \\ & + \beta_1\alpha_2|V\rangle_1|H\rangle_4|V\rangle_{5'} + \alpha_1\alpha_2|H\rangle_1|H\rangle_4|H\rangle_{5''} - \alpha_1\alpha_2|H\rangle_1|H\rangle_4|V\rangle_{5''} \\ & - \beta_1\alpha_2|V\rangle_1|H\rangle_4|H\rangle_{5''} + \beta_1\alpha_2|V\rangle_1|H\rangle_4|V\rangle_{5''}) \\ & \otimes (|H\rangle_{a_2} + |V\rangle_{a_2}) \otimes (\alpha_3|H\rangle_{t_{in}} + \beta_3|V\rangle_{t_{in}}). \end{aligned} \quad (19)$$

If D_{H_6} is triggered, the photon emitted from spatial mode $5'$ is led to PBS₅ to mix with the photon emitted from mode a_2 , Eq. (19) will collapse into the state

$$\begin{aligned} |\Psi_4\rangle = & \frac{1}{\sqrt{2}}(\alpha_1\alpha_2|H\rangle_1|H\rangle_4 + \alpha_1\beta_2|H\rangle_1|V\rangle_{5'} + \beta_1\alpha_2|V\rangle_1|H\rangle_4 + \beta_1\beta_2|V\rangle_1|H\rangle_{5'}) \\ & \otimes (|H\rangle_{a_2} + |V\rangle_{a_2}) \otimes (\alpha_3|H\rangle_{t_{in}} + \beta_3|V\rangle_{t_{in}}), \end{aligned} \quad (20)$$

with a probability of $\frac{1}{2} \times \frac{1+\alpha_2^2}{2} \times \frac{1}{4}$. If D_{V_6} is triggered, the photon emitted from spatial mode $5'$ will be applied a feedback σ_x operation to convert the state

$$\begin{aligned} |\Psi'_4\rangle = & \frac{1}{\sqrt{2}}(\alpha_1\alpha_2|H\rangle_1|H\rangle_4 + \alpha_1\beta_2|H\rangle_1|H\rangle_{5'} + \beta_1\alpha_2|V\rangle_1|H\rangle_4 + \beta_1\beta_2|V\rangle_1|V\rangle_{5'}) \\ & \otimes (|H\rangle_{a_2} + |V\rangle_{a_2}) \otimes (\alpha_3|H\rangle_{t_{in}} + \beta_3|V\rangle_{t_{in}}), \end{aligned} \quad (21)$$

with a probability of $\frac{1}{2} \times \frac{1+\alpha_2^2}{2} \times \frac{1}{4}$ to Eq. (20). The σ_x operation can be achieved easily by an HWP $^{45^\circ}$ setting in mode $5'$.

In the third step, after PBS₅ completes the parity-check measurement on the photons emitted from spatial modes $5'$ and a_2 , the instance in which the spatial mode 8 involves exactly one photon is chosen, and then the system will be in the following normalization state

$$\begin{aligned} |\Psi_5\rangle = & (\alpha_1\alpha_2|H\rangle_1|H\rangle_4|V\rangle_8 + \alpha_1\beta_2|H\rangle_1|V\rangle_7|V\rangle_8 + \beta_1\alpha_2|V\rangle_1|H\rangle_4|V\rangle_8 \\ & + \beta_1\beta_2|V\rangle_1|H\rangle_7|H\rangle_8) \otimes (\alpha_3|H\rangle_{t_{in}} + \beta_3|V\rangle_{t_{in}}), \end{aligned} \quad (22)$$

with a probability of $\frac{1}{2} \times \frac{1+\alpha_2^2}{2} \times (\frac{1}{4} + \frac{1}{4}) \times \frac{1}{2}$.

In the fourth step, the photons emitted from spatial modes 7 and 4 pass through HWP $^{67.5^\circ}$ and HWP $^{22.5^\circ}$ respectively, and then are fed into PBS₈. Before and after the photons emitted from spatial modes 8 and t_{in} mix at PBS₆, four HWP $^{22.5^\circ}$'s are performed on them. The even-parity is chosen for the polarized photons in modes 11 and 12 after PBS₆. Therefore, before $D_{H_{12}}$ or $D_{V_{12}}$ is fired, these elements induce the outing photons in the state

$$\begin{aligned}
 |\Psi_6\rangle = & \frac{1}{2}(\gamma_1|H\rangle_1|H\rangle_9|H\rangle_{11} + \gamma_2|H\rangle_1|H\rangle_9|V\rangle_{11} + \gamma_3|H\rangle_1|V\rangle_9|H\rangle_{11} \\
 & + \gamma_4|H\rangle_1|V\rangle_9|V\rangle_{11} + \gamma_5|V\rangle_1|H\rangle_9|H\rangle_{11} + \gamma_6|V\rangle_1|H\rangle_9|V\rangle_{11} \\
 & + \gamma_7|V\rangle_1|V\rangle_9|V\rangle_{11} + \gamma_8|V\rangle_1|V\rangle_9|H\rangle_{11}) \otimes |V\rangle_{12} \\
 & + \frac{1}{2}(\gamma_1|H\rangle_1|H\rangle_9|V\rangle_{11} + \gamma_2|H\rangle_1|H\rangle_9|H\rangle_{11} + \gamma_3|H\rangle_1|V\rangle_9|V\rangle_{11} \\
 & + \gamma_4|H\rangle_1|V\rangle_9|H\rangle_{11} + \gamma_5|V\rangle_1|H\rangle_9|V\rangle_{11} + \gamma_6|V\rangle_1|H\rangle_9|H\rangle_{11} \\
 & + \gamma_7|V\rangle_1|V\rangle_9|H\rangle_{11} + \gamma_8|V\rangle_1|V\rangle_9|V\rangle_{11}) \otimes |H\rangle_{12} \\
 & + \frac{1}{2}(\gamma_1|H\rangle_1|V\rangle_{10}|H\rangle_{11} + \gamma_2|H\rangle_1|V\rangle_{10}|V\rangle_{11} + \gamma_3|H\rangle_1|H\rangle_{10}|H\rangle_{11} \\
 & + \gamma_4|H\rangle_1|H\rangle_{10}|V\rangle_{11} + \gamma_5|V\rangle_1|V\rangle_{10}|H\rangle_{11} + \gamma_6|V\rangle_1|V\rangle_{10}|V\rangle_{11} \\
 & - \gamma_7|V\rangle_1|H\rangle_{10}|V\rangle_{11} - \gamma_8|V\rangle_1|H\rangle_{10}|H\rangle_{11}) \otimes |V\rangle_{12} \\
 & + \frac{1}{2}(\gamma_1|H\rangle_1|V\rangle_{10}|V\rangle_{11} + \gamma_2|H\rangle_1|V\rangle_{10}|H\rangle_{11} + \gamma_3|H\rangle_1|H\rangle_{10}|V\rangle_{11} \\
 & + \gamma_4|H\rangle_1|H\rangle_{10}|H\rangle_{11} + \gamma_5|V\rangle_1|V\rangle_{10}|V\rangle_{11} + \gamma_6|V\rangle_1|V\rangle_{10}|H\rangle_{11} \\
 & - \gamma_7|V\rangle_1|H\rangle_{10}|H\rangle_{11} - \gamma_8|V\rangle_1|H\rangle_{10}|V\rangle_{11}) \otimes |H\rangle_{12},
 \end{aligned} \tag{23}$$

with a probability of $\frac{1}{2} \times \frac{1+\alpha_2^2}{2} \times (\frac{1}{4} + \frac{1}{4}) \times \frac{1}{2} \times \frac{1}{2}$. Here, for simplicity, the coefficients are written as $\gamma_1 = \alpha_1\alpha_2\alpha_3$, $\gamma_2 = \alpha_1\alpha_2\beta_3$, $\gamma_3 = \alpha_1\beta_2\alpha_3$, $\gamma_4 = \alpha_1\beta_2\beta_3$, $\gamma_5 = \beta_1\alpha_2\alpha_3$, $\gamma_6 = \beta_1\alpha_2\beta_3$, $\gamma_7 = \beta_1\beta_2\alpha_3$, and $\gamma_8 = \beta_1\beta_2\beta_3$. Half-wave plate HWP $^{67.5^\circ}$ induces the transformations

$$|H\rangle \xrightarrow{\text{HWP}^{67.5^\circ}} \frac{1}{\sqrt{2}}(|V\rangle - |H\rangle), \quad |V\rangle \xrightarrow{\text{HWP}^{67.5^\circ}} \frac{1}{\sqrt{2}}(|H\rangle + |V\rangle). \tag{24}$$

Based on Eq. (23), one can see that when $D_{V_{12}}$ is fired, the outing photons from the spatial modes 1, 9, and 11 kept are in the state

$$\begin{aligned}
 |\Psi_7\rangle = & \gamma_1|H\rangle_1|H\rangle_9|H\rangle_{11} + \gamma_2|H\rangle_1|H\rangle_9|V\rangle_{11} + \gamma_3|H\rangle_1|V\rangle_9|H\rangle_{11} + \gamma_4|H\rangle_1|V\rangle_9|V\rangle_{11} \\
 & + \gamma_5|V\rangle_1|H\rangle_9|H\rangle_{11} + \gamma_6|V\rangle_1|H\rangle_9|V\rangle_{11} + \gamma_7|V\rangle_1|V\rangle_9|V\rangle_{11} + \gamma_8|V\rangle_1|V\rangle_9|H\rangle_{11},
 \end{aligned} \tag{25}$$

with a probability of $\frac{1}{2} \times \frac{1+\alpha_2^2}{2} \times (\frac{1}{4} + \frac{1}{4}) \times \frac{1}{2} \times \frac{1}{2} \times \frac{1}{4}$. That is, the probabilistic Toffoli gate is completed.

When $D_{H_{12}}$ is fired, the outing photons from the spatial modes 1, 9, and 11 kept are in the state

$$\begin{aligned}
 |\Psi'_7\rangle = & \gamma_1|H\rangle_1|H\rangle_9|V\rangle_{11} + \gamma_2|H\rangle_1|H\rangle_9|H\rangle_{11} + \gamma_3|H\rangle_1|V\rangle_9|V\rangle_{11} + \gamma_4|H\rangle_1|V\rangle_9|H\rangle_{11} \\
 & + \gamma_5|V\rangle_1|H\rangle_9|V\rangle_{11} + \gamma_6|V\rangle_1|H\rangle_9|H\rangle_{11} + \gamma_7|V\rangle_1|V\rangle_9|H\rangle_{11} + \gamma_8|V\rangle_1|V\rangle_9|V\rangle_{11},
 \end{aligned} \tag{26}$$

with a probability of $\frac{1}{2} \times \frac{1+\alpha_2^2}{2} \times (\frac{1}{4} + \frac{1}{4}) \times \frac{1}{2} \times \frac{1}{2} \times \frac{1}{4}$. To complete the Toffoli gate, a feed-forward σ_x operation is applied to photon in spatial mode 11. The outcomes of measurement

Table 1: Measurement outcomes and corresponding feed-forward operations in mode 5' or 11 for realizing a Toffoli gate. I_2 is an identity operation and σ_x is a Pauli X operation, which can be realized by an HWP setting at 45° .

Measurement		Feed-forward		Achieved result
Detector	Detector	mode 5'	mode 11	
D_{H_6}	$D_{V_{12}}$	I_2	I_2	Toffoli
D_{H_6}	$D_{H_{12}}$	I_2	σ_x	Toffoli
D_{V_6}	$D_{V_{12}}$	σ_x	I_2	Toffoli
D_{V_6}	$D_{H_{12}}$	σ_x	σ_x	Toffoli

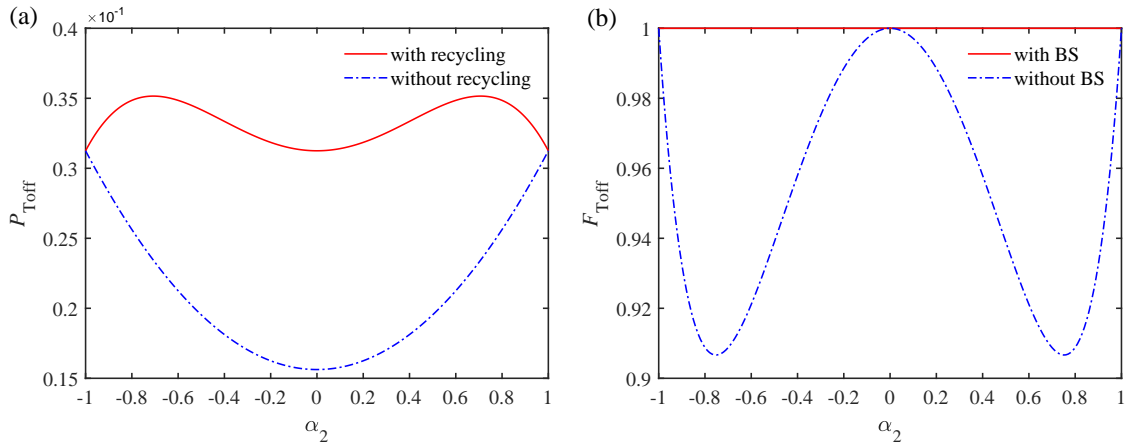


Figure 3: (a) The relations between the success probability of Toffoli gate (P_{Toff}) and parameter α_2 with/without recycling. The blue dashed curve indicates $P_{\text{Toff}} = \frac{1+\alpha_2^2}{64}$ without recycling the photons in mode 5'', while the red solid curve indicates $P_{\text{Toff}} = \frac{(1+\alpha_2^2)(2-\alpha_2^2)}{64}$ with recycling the photons in mode 5''. (b) The relations between the fidelity of Toffoli gate (F_{Toff}) and parameter α_2 with/without BS. The blue dashed and red solid curves indicate the fidelity of the Toffoli gate without and with BS, respectively.

and corresponding feed-forward operations for completing Toffoli gate are summarized in Tab. 1. When D_{10} is fired, it means that the scheme fails.

We evaluate the performance of the scheme by characterizing success probability and fidelity of Toffoli gate, respectively. The success probability of Toffoli gate is defined as $P_{\text{Toff}} = n_{\text{out}}/n_{\text{in}}$, where n_{out} and n_{in} are the number of output photon and input photon, respectively. The fidelity of Toffoli gate is defined as $F_{\text{Toff}} = |\langle \varphi_{\text{real}} | \varphi_{\text{ideal}} \rangle|$, where φ_{real} and φ_{ideal} are the real normalized output state of the gate and ideal normalized output state of the gate, respectively. The quantum circuit shown in Fig. 2 completed a post-selection Toffoli gate with a success probability of $P_{\text{Toff}} = \frac{1}{2} \times \frac{1+\alpha_2^2}{2} \times \frac{1}{2} \times \frac{1}{2} \times \frac{1}{2} \times \frac{1}{2} = \frac{1+\alpha_2^2}{64}$ and unity fidelity in principle. Alternately, the success probability of the gate with unity fidelity can be further enhanced to $\frac{1}{2} \times \frac{1+\alpha_2^2}{2} \times \frac{2-\alpha_2^2}{2} \times \frac{1}{2} \times \frac{1}{2} \times \frac{1}{2} = \frac{(1+\alpha_2^2)(2-\alpha_2^2)}{64}$ by recycling the photons emitted from spatial mode 5'' into the PBS₅ because the state has the same form as the state shown in Eq. (20). From Fig. 3(a), one can see that the minimum P_{Toff} without recycling is approximately $\frac{1}{64}$, the maximum P_{Toff} without recycling reaches approximately $\frac{1}{32}$, and the average P_{Toff}

without recycling is $\frac{1}{2} \int_{-1}^1 \frac{1+\alpha_2^2}{64} d\alpha_2 = \frac{1}{48}$. In contrast, with recycling one, the minimum P_{Toff} is approximately $\frac{1}{32}$, the maximum P_{Toff} can reach $\frac{9}{256}$, and the average P_{Toff} is $\frac{1}{30}$. The success probability of our Toffoli gate is much higher than previous works [53–57]. As shown in Fig. 3(b), if the BS is discarded in Fig. 2, the fidelity of Toffoli gate will reduce from unity (red solid curve) to $F_{\text{Toff}} = 1 - \alpha_2^2 + \frac{\alpha_2^2}{\sqrt{2-\alpha_2^2}}$ (blue dashed curve), and the success probability will be $P_{\text{Toff}} = \frac{(1+\alpha_2^2)(2-\alpha_2^2)}{64}$, which is higher than the without recycling one and equals to the with recycling one. From Fig. 3(b), one can see that the fidelity of the Toffoli gate keeps unity for the scheme with BS in principle, while the average fidelity of the Toffoli gate over α_2 is $\frac{3\pi+2}{12} \approx 95.2\%$ for the scheme without BS.

Table 2: A comparison of proposed post-selected CPF gate with linear optics and previous schemes.

Proposed schemes	Ancillary photons	Success probability	Achieved results
Refs. [25–29]	A Bell-state	1/4	CNOT
Refs. [30–32]	No	1/9	CPF
Refs. [33–35]	No	1/9	CNOT
Refs. [36, 37]	Two single photons	1/8	CNOT
Ref. [38]	Two single photons	1/16	CNOT
Ref. [56]	No	1/8	CNOT
Ref. [57]	No	1/9	CNOT
This work	A single photon	1/4	CPF

Table 3: A comparison of proposed post-selected Toffoli gate with linear optics and previous schemes.

Proposed schemes	Ancillary photons	Success probability
Fiurášek [53]	No	1/133
Ralph <i>et al.</i> [54]	No	1/72
Ralph <i>et al.</i> [54]	Two Bell-states	1/32
Lanyon <i>et al.</i> [55]	No	1/72
Liu <i>et al.</i> [56]	No	1/64
Li <i>et al.</i> [57]	No	1/60
This work	Two single photons	1/30

4 Conclusion

We have proposed two schemes to implement post-selected CPF and Toffoli gates in the coincidence basis by solely using linear optics. The comparisons between our proposed CPF gate and Toffoli gate and previous schemes are presented in Tab. 2 and Tab. 3, respectively. A maximally entangled photon pair [25–29] (or two single photons [36, 37]) is necessary for implementing a CNOT gate with the current existing maximum success probability of 1/4 (or

$1/8$). Only one auxiliary single photon is introduced to accomplish our CPF gate with the success probability of $1/4$. In addition, our approach to implement Toffoli gate is much more efficient than the synthesis one. Assisted by two independent single photons, our Toffoli gate is constructed with the current maximum success probability of $1/30$.

We note that the success condition of the gates can only be verified by the final detection of outing photons using the photon-number-resolving detector (PNRD) [64–66]. This coincidence basis operation without quantum nondemolition detection causes an unscalable approach to the construction of quantum gate, but it provides a convenient means of experimental test of optical CPF gate and Toffoli gate. The PNRD can distinguish the number of photons, which is an important resource for many quantum information processing tasks realized in experiments [29, 36, 37, 67]. Our presented two architectures open an alternative insight into probabilistic quantum gates using linear optical elements and suggest that they maybe have various applications in photonic quantum information processing.

Acknowledgments

This work was supported by the National Natural Science Foundation of China under Grant No. 11604012, the Fundamental Research Funds for the Central Universities under Grants FRF-TP-19-011A3.

References

- [1] M. A. Nielsen and I. L. Chuang, *Quantum Computation and Quantum Information: 10th Anniversary Edition*, Cambridge University Press, doi:10.1017/CBO9780511976667 (2010).
- [2] A. Barenco, C. H. Bennett, R. Cleve, D. P. DiVincenzo, N. Margolus, P. Shor, T. Sleator, J. A. Smolin and H. Weinfurter, *Elementary gates for quantum computation*, Phys. Rev. A **52**, 3457 (1995), doi:10.1103/PhysRevA.52.3457.
- [3] M. Möttönen, J. J. Vartiainen, V. Bergholm and M. M. Salomaa, *Quantum circuits for general multiqubit gates*, Phys. Rev. Lett. **93**, 130502 (2004), doi:10.1103/PhysRevLett.93.130502.
- [4] W. Q. Liu and H. R. Wei, *Optimal synthesis of the Fredkin gate in a multilevel system*, New J. Phys. **22**, 063026 (2020), doi:10.1088/1367-2630/ab8e13.
- [5] W. Q. Liu, H. R. Wei and L. C. Kwek, *Low-cost Fredkin gate with auxiliary space*, Phys. Rev. Appl. **14**, 054057 (2020), doi:10.1103/PhysRevApplied.14.054057.
- [6] A. S. Nikolaeva, E. O. Kiktenko and A. K. Fedorov, *Decomposing the generalized Toffoli gate with qutrits*, Phys. Rev. A **105**, 032621 (2022).
- [7] L. K. Grover, *Quantum mechanics helps in searching for a needle in a haystack*, Phys. Rev. Lett. **79**, 325 (1997), doi:10.1103/PhysRevLett.79.325.

- [8] P. W. Shor, *Polynomial-time algorithms for prime factorization and discrete logarithms on a quantum computer*, SIAM Rev. **41**, 303 (1999), doi:10.1137/S0036144598347011.
- [9] K. Bharti, A. Cervera-Lierta, T. H. Kyaw, T. Haug, S. Alperin-Lea, A. Anand, M. Degroote, H. Heimonen, J. S. Kottmann, T. Menke *et al.*, *Noisy intermediate-scale quantum algorithms*, Rev. Mod. Phys. **94**, 015004 (2022), doi:10.1103/RevModPhys.94.015004.
- [10] I. M. Georgescu, S. Ashhab and F. Nori, *Quantum simulation*, Rev. Mod. Phys. **86**, 153 (2014), doi:10.1103/RevModPhys.86.153.
- [11] B. X. Wang, M. J. Tao, Q. Ai, T. Xin, N. Lambert, D. Ruan, Y. C. Cheng, F. Nori, F. G. Deng and G. L. Long, *Efficient quantum simulation of photosynthetic light harvesting*, npj Quantum Inf. **4**, 52 (2018), doi:10.1038/s41534-018-0102-2.
- [12] W. T. He, H. Y. Guang, Z. Y. Li, R. Q. Deng, N. N. Zhang, J. X. Zhao, F. G. Deng and Q. Ai, *Quantum metrology with one auxiliary particle in a correlated bath and its quantum simulation*, Phys. Rev. A **104**, 062429 (2021), doi:10.1103/PhysRevA.104.062429.
- [13] J. W. Pan, Z. B. Chen, C. Y. Lu, H. Weinfurter, A. Zeilinger and M. Żukowski, *Multiphoton entanglement and interferometry*, Rev. Mod. Phys. **84**, 777 (2012), doi:10.1103/RevModPhys.84.777.
- [14] G. L. Long, *General quantum interference principle and duality computer*, Commun. Theor. Phys. **45**, 825 (2006), doi:10.1088/0253-6102/45/5/013.
- [15] X. Zou, D. Qiu, L. Wu, L. Li and L. Li, *On mathematical theory of the duality computers*, Quantum Inf. Process. **8**, 37 (2009), doi:10.1007/s11128-008-0093-6.
- [16] S. J. Wei and G. L. Long, *Duality quantum computer and the efficient quantum simulations*, Quantum Inf. Process. **15**, 1189 (2016), doi:10.1007/s11128-016-1263-6.
- [17] X. X. Hu, F. H. Zhang, Y. S. Li and G. L. Long, *Optimizing quantum gates within decoherence-free subspaces*, Phys. Rev. A **104**, 062612 (2021), doi:10.1103/PhysRevA.104.062612.
- [18] J. L. O'Brien, *Optical quantum computing*, Science **318**, 1567 (2007), doi:10.1126/science.1142892.
- [19] P. Kok, W. J. Munro, K. Nemoto, T. C. Ralph, J. P. Dowling and G. J. Milburn, *Linear optical quantum computing with photonic qubits*, Rev. Mod. Phys. **79**, 135 (2007), doi:10.1103/RevModPhys.79.135.
- [20] E. Knill, R. Laflamme and G. J. Milburn, *A scheme for efficient quantum computation with linear optics*, Nature **409**, 46 (2001), doi:10.1038/35051009.
- [21] X. Li, Y. Wu, D. Steel, D. Gammon, T. H. Stievater, D. S. Katzer, D. Park, C. Piermarocchi and L. J. Sham, *An all-optical quantum gate in a semiconductor quantum dot*, Science **301**, 809 (2003), doi:10.1126/science.1083800.
- [22] H. R. Wei and F. G. Deng, *Compact quantum gates on electron-spin qubits assisted by diamond nitrogen-vacancy centers inside cavities*, Phys. Rev. A **88**, 042323 (2013), doi:10.1103/PhysRevA.88.042323.

- [23] I. I. Beterov, I. N. Ashkarin, E. A. Yakshina, D. B. Tretyakov, V. M. Entin, I. I. Ryabtsev, P. Cheinet, P. Pillet and M. Saffman, *Fast three-qubit Toffoli quantum gate based on three-body Förster resonances in Rydberg atoms*, Phys. Rev. A **98**, 042704 (2018), doi:10.1103/PhysRevA.98.042704.
- [24] T. C. Ralph, A. G. White, W. J. Munro and G. J. Milburn, *Simple scheme for efficient linear optics quantum gates*, Phys. Rev. A **65**, 012314 (2001), doi:10.1103/PhysRevA.65.012314.
- [25] T. B. Pittman, B. C. Jacobs and J. D. Franson, *Probabilistic quantum logic operations using polarizing beam splitters*, Phys. Rev. A **64**, 062311 (2001), doi:10.1103/PhysRevA.64.062311.
- [26] T. B. Pittman, B. C. Jacobs and J. D. Franson, *Demonstration of nondeterministic quantum logic operations using linear optical elements*, Phys. Rev. Lett. **88**, 257902 (2002), doi:10.1103/PhysRevLett.88.257902.
- [27] S. Gasparoni, J. W. Pan, P. Walther, T. Rudolph and A. Zeilinger, *Realization of a photonic controlled-NOT gate sufficient for quantum computation*, Phys. Rev. Lett. **93**, 020504, doi:10.1103/PhysRevLett.93.020504.
- [28] Z. Zhao, A. N. Zhang, Y. A. Chen, H. Zhang, J. F. Du, T. Yang and J. W. Pan, *Experimental demonstration of a nondestructive controlled-NOT quantum gate for two independent photon qubits*, Phys. Rev. Lett. **94**, 030501 (2005), doi:10.1103/PhysRevLett.94.030501.
- [29] J. Zeuner, A. N. Sharma, M. Tillmann, R. Heilmann, M. Gräfe, A. Moqanaki, A. Szameit and P. Walther, *Integrated-optics heralded controlled-NOT gate for polarization-encoded qubits*, npj Quantum Inf. **4**, 13 (2018), doi:10.1038/s41534-018-0068-0.
- [30] H. F. Hofmann and S. Takeuchi, *Quantum phase gate for photonic qubits using only beam splitters and postselection*, Phys. Rev. A **66**, 024308 (2002), doi:10.1103/PhysRevA.66.024308.
- [31] N. K. Langford, T. J. Weinhold, R. Prevedel, K. J. Resch, A. Gilchrist, J. L. O'Brien, G. J. Pryde and A. G. White, *Demonstration of a simple entangling optical gate and its use in Bell-state analysis*, Phys. Rev. Lett. **95**, 210504 (2005), doi:10.1103/PhysRevLett.95.210504.
- [32] N. Kiesel, C. Schmid, U. Weber, R. Ursin and H. Weinfurter, *Linear optics controlled-phase gate made simple*, Phys. Rev. Lett. **95**, 210505 (2005), doi:10.1103/PhysRevLett.95.210505.
- [33] J. L. O'Brien, G. J. Pryde, A. G. White, T. C. Ralph and D. Branning, *Demonstration of an all-optical quantum controlled-NOT gate*, Nature **426**, 264 (2003), doi:10.1038/nature02054.
- [34] R. Okamoto, H. F. Hofmann, S. Takeuchi and K. Sasaki, *Demonstration of an optical quantum controlled-NOT gate without path interference*, Phys. Rev. Lett. **95**, 210506, doi:10.1103/PhysRevLett.95.210506.

- [35] Y. M. He, Y. He, Y. J. Wei, D. Wu, M. Atatüre, C. Schneider, S. Höfling, M. Kamp, C. Y. Lu and J. W. Pan, *On-demand semiconductor single-photon source with near-unity indistinguishability*, Nat. Nanotechnol. **8**, 213 (2013), doi:10.1038/nnano.2012.262.
- [36] X. H. Bao, T. Y. Chen, Q. Zhang, J. Yang, H. Zhang, T. Yang and J. W. Pan, *Optical nondestructive controlled-NOT gate without using entangled photons*, Phys. Rev. Lett. **98**, 170502 (2007), doi:10.1103/PhysRevLett.98.170502.
- [37] J. P. Li, X. Gu, J. Qin, D. Wu, X. You, H. Wang, C. Schneider, S. Höfling, Y. H. Huo, C. Y. Lu *et al.*, *Heralded nondestructive quantum entangling gate with single-photon sources*, Phys. Rev. Lett. **126**, 140501 (2021), doi:10.1103/PhysRevLett.126.140501.
- [38] R. Okamoto, J. L. O'Brien, H. F. Hofmann and S. Takeuchi, *Realization of a Knill-Laflamme-Milburn controlled-NOT photonic quantum circuit combining effective optical nonlinearities*, Proc. Natl. Acad. Sci. U.S.A. **108**, 10067 (2011), doi:10.1073/pnas.1018839108.
- [39] S. U. Shringarpure and J. D. Franson, *Proposal for a destructive controlled phase gate using linear optics*, Sci. Rep. **11**, 22067 (2021), doi:10.1038/s41598-021-01384-2.
- [40] J. H. Plantenberg, P. C. De Groot, C. J. P. M. Harmans and J. E. Mooij, *Demonstration of controlled-NOT quantum gates on a pair of superconducting quantum bits*, Nature **447**, 836 (2007), doi:10.1038/nature05896.
- [41] L. Isenhower, E. Urban, X. L. Zhang, A. T. Gill, T. Henage, T. A. Johnson, T. G. Walker and M. Saffman, *Demonstration of a neutral atom controlled-NOT quantum gate*, Phys. Rev. Lett. **104**, 010503 (2010), doi:10.1103/PhysRevLett.104.010503.
- [42] Y. Wan, D. Kienzler, S. D. Erickson, K. H. Mayer, T. R. Tan, J. J. Wu, H. M. Vasconcelos, S. Glancy, E. Knill, D. J. Wineland *et al.*, *Quantum gate teleportation between separated qubits in a trapped-ion processor*, Science **364**, 875 (2019), doi:10.1126/science.aaw941.
- [43] C. Couteau, *Spontaneous parametric down-conversion*, Contemp. Phys. **59**, 291 (2018), doi:10.1080/00107514.2018.1488463.
- [44] L. M. K. Vandersypen, M. Steffen, G. Breyta, C. S. Yannoni, M. H. Sherwood and I. L. Chuang, *Experimental realization of Shor's quantum factoring algorithm using nuclear magnetic resonance*, Nature **414**, 883 (2001), doi:10.1038/414883a.
- [45] K. A. Brickman, P. C. Haljan, P. J. Lee, M. Acton, L. Deslauriers and C. Monroe, *Implementation of Grover's quantum search algorithm in a scalable system*, Phys. Rev. A **72**, 050306(R) (2005), doi:10.1103/PhysRevA.72.050306.
- [46] G. A. Barbosa, *Quantum half-adder*, Phys. Rev. A **73**, 052321 (2006), doi:10.1103/PhysRevA.73.052321.
- [47] D. G. Cory, M. D. Price, W. Maas, E. Knill, R. Laflamme, W. H. Zurek, T. F. Havel and S. S. Somaroo, *Experimental quantum error correction*, Phys. Rev. Lett. **81**, 2152 (1998), doi:10.1103/PhysRevLett.81.2152.

- [48] A. Paetznick and B. W. Reichardt, *Universal fault-tolerant quantum computation with only transversal gates and error correction*, Phys. Rev. Lett. **111**, 090505 (2013), doi:10.1103/PhysRevLett.111.090505.
- [49] T. Monz, K. Kim, W. Hänsel, M. Riebe, A. S. Villar, P. Schindler, M. Chwalla, M. Hennrich and R. Blatt, *Realization of the quantum Toffoli gate with trapped ions*, Phys. Rev. Lett. **102**, 040501 (2009), doi:10.1103/PhysRevLett.102.040501.
- [50] A. Fedorov, L. Steffen, M. Baur, M. P. da Silva and A. Wallraff, *Implementation of a Toffoli gate with superconducting circuits*, Nature **481**, 170 (2012), doi:10.1038/nature10713.
- [51] H. Levine, A. Keesling, G. Semeghini, A. Omran, T. T. Wang, S. Ebadi, H. Bernien, M. Greiner, V. Vuletić, H. Pichler *et al.*, *Parallel implementation of high-fidelity multiqubit gates with neutral atoms*, Phys. Rev. Lett. **123**, 170503 (2019), doi:10.1103/PhysRevLett.123.170503.
- [52] N. Yu, R. Duan and M. Ying, *Five two-qubit gates are necessary for implementing the Toffoli gate*, Phys. Rev. A **88**, 010304(R) (2013), doi:10.1103/PhysRevA.88.010304.
- [53] J. Fiurášek, *Linear-optics quantum Toffoli and Fredkin gates*, Phys. Rev. A **73**, 062313 (2006), doi:10.1103/PhysRevA.73.062313.
- [54] T. C. Ralph, K. J. Resch and A. Gilchrist, *Efficient Toffoli gates using qudits*, Phys. Rev. A **75**, 022313 (2007), doi:10.1103/PhysRevA.75.022313.
- [55] B. P. Lanyon, M. Barbieri, M. P. Almeida, T. Jennewein, T. C. Ralph, K. J. Resch, G. J. Pryde, J. L. O'Brien, A. Gilchrist and A. G. White, *Simplifying quantum logic using higher-dimensional Hilbert spaces*, Nat. Phys. **5**, 134 (2009), doi:10.1038/nphys1150.
- [56] W. Q. Liu, H. R. Wei and L. C. Kwek, *Universal quantum multi-qubit entangling gates with auxiliary spaces*, Adv. Quantum Technol. **5**, 2100136 (2022), doi:10.1002/qute.202100136.
- [57] Y. Li, L. Wan, H. Zhang, H. Zhu, Y. Shi, L. K. Chin, X. Zhou, L. C. Kwek and A. Q. Liu, *Quantum Fredkin and Toffoli gates on a versatile programmable silicon photonic chip*, npj Quantum Inf. **8**, 112 (2022), doi:10.1038/s41534-022-00627-y.
- [58] M. Li, C. Li, Y. Chen, L. T. Feng, L. Yan, Q. Zhang, J. Bao, B. H. Liu, X. F. Ren, J. Wang *et al.*, *On-chip path encoded photonic quantum Toffoli gate*, Photon. Res. **10**, 07001533 (2022), doi:10.1364/PRJ.452539.
- [59] M. Mičuda, M. Sedlák, I. Straka, M. Miková, M. Dušek, M. Ježek and J. Fiurášek, *Efficient experimental estimation of fidelity of linear optical quantum Toffoli gate*, Phys. Rev. Lett. **111**, 160407 (2013), doi:10.1103/PhysRevLett.111.160407.
- [60] M. Mičuda, M. Miková, I. Straka, M. Sedlák, M. Dušek, M. Ježek and J. Fiurášek, *Tomographic characterization of a linear optical quantum Toffoli gate*, Phys. Rev. A **92**, 032312 (2015), doi:10.1103/PhysRevA.92.032312.
- [61] Q. Zeng, T. Li, X. Song and X. Zhang, *Realization of optimized quantum controlled-logic gate based on the orbital angular momentum of light*, Opt. Express **24**, 8186 (2016), doi:10.1364/OE.24.008186.

- [62] H. L. Huang, W. S. Bao, T. Li, F. G. Li, X. Q. Fu, S. Zhang, H. L. Zhang and X. Wang, *Deterministic linear optical quantum Toffoli gate*, Phys. Lett. A **381**, 2673 (2017), doi:10.1016/j.physleta.2017.06.034.
- [63] S. Ru, Y. Wang, M. An, F. Wang, P. Zhang and F. Li, *Realization of a deterministic quantum Toffoli gate with a single photon*, Phys. Rev. A **103**, 022606 (2021), doi:10.1103/PhysRevA.103.022606.
- [64] M. J. Fitch, B. C. Jacobs, T. B. Pittman and J. D. Franson, *Photon-number resolution using time-multiplexed single-photon detectors*, Phys. Rev. A **68**, 043814 (2003), doi:10.1103/PhysRevA.68.043814.
- [65] A. Divochiy, F. Marsili, D. Bitauld, A. Gaggero, R. Leoni, F. Mattioli, A. Korneev, V. Seleznev, N. Kaurova, O. Minaeva *et al.*, *Superconducting nanowire photon-number-resolving detector at telecommunication wavelengths*, Nat. Photonics **2**, 302 (2008), doi:10.1038/nphoton.2008.51.
- [66] R. Nehra, C. H. Chang, Q. Yu, A. Beling and O. Pfister, *Photon-number-resolving segmented detectors based on single-photon avalanche-photodiodes*, Opt. Express **28**, 3660 (2020), doi:10.1364/OE.380416.
- [67] J. W. Pan, C. Simon, Č. Brukner and A. Zeilinger, *Entanglement purification for quantum communication*, Nature **410**, 1067 (2001), doi:10.1038/35074041.